FLOMEKO 2022

Design of Flow Conditioner and Research on Evaluation of Flow Adjustment Effect

W. L. Chen[1,2], C. H. Li[3], and X. Y. Li[2]

[1] College of Civil Engineering and Mechanics, Lanzhou University, Lanzhou, China;
[2] Xinjiang Institute of Measurement & Testing Technology, No. 188, hebei east road, xinshi district, Urumqi, China
[3] National Institute of Metrology, Beijing, China
E-mail: chenwl16@lzu.edu.cn

Abstract

Since ultrasonic flowmeter is sensitive to the flow field. Insufficient development of the flow field such as vortex and asymmetric flow will cause deviations in the measurement results. It has become a common method to accelerate the stabilization of irregular fluids to a fully developed state by a flow conditioner. The flow conditioner is a device installed upstream of the flowmeter to accelerate the stabilization of the irregular flow field, eliminate abnormal flow, and reduce the influence of swirling flow.

In practical application, the correlation between flow conditioner and flow meter model has also become an important obstacle restricting the design, compatibility and popularization of flow conditioner. It is an exploratory and meaningful work to design a universal flow conditioner and propose a flow field optimization evaluation method and other basic theories and common key technologies of flow measurement.

This paper introduces the self-designed universal flow conditioner, and focuses on the flow adjustment effect evaluation method based on CFD.

In order to verify the adjustment effect of the combined flow conditioner, the simulated calculation is carried out and the flow field adjustment effect is compared with that of the plate-type flow conditioner.When the inlet flow rate is 20 m/s, the simulation results show that the combined flow conditioner has excellent performance in eliminating flow field distortion at about 15D downstream the flow conditioner, while the flow velocity distribution in the axial direction can also be optimized to a fully developed symmetrical state.

1. Introduction

In the design process of ultrasonic flowmeter, the purpose of flow field analysis and supplementary methods is to improve the measurement accuracy and flow field adaptability of the flowmeter[1]. There are usually two methods. One is to analyze the flow field where the ultrasonic flowmeter is located by means of real flow calibration or numerical simulation, to obtain the relationship between the different pipe sections upstream of the flowmeter and the corresponding measurement error, and to improve the algorithm to obtain the corresponding measurement error compensation method[2]. The other is to consider that the measurement of the ideal ultrasonic flowmeter requires an axisymmetric flow pattern, and there is no non-ideal flow field such as radial component, secondary flow, local turbulence, etc. Therefore, the flow conditioner (FC), which is a device installed upstream of the flow meter to accelerate the stabilization of the irregular flow field, eliminate abnormal flow, and reduce the influence of swirling flow[3], are used to obtain a fully developed flow field.

At present, all kinds of ultrasonic flowmeters on the market have FC that are used together with them. The specificity of FC is relatively strong, and the applicability analysis of FCs with different structures to different flow types is still lacking[4].

The combined FC generally consists of a front-end member for initial rectification of irregular flows, a buffer chamber, and a back-end member for achieving a fully axisymmetric and fully developed velocity distribution over a short distance[5]. Existing combined FCs generally use vane type and perforated plate type FCs as front and rear components. However, this type of FC has a complex structure, requires high machining accuracy, and involves many parameters. If the FC is designed and optimized using the parameter-by-parameter analysis method, a large number of complicated tests are required, and the process is cumbersome and time-consuming[6].

In view of this situation, this paper designs a universal combined FC. And a flow field evaluation method is proposed to evaluate the rectification effect of the FC.

2. Structural design of combined FC

The combined FC is divided into a front filter buffer cavity and a back-end rectifier cavity. The total length of the filter buffer chamber is 1D, and the total length of the rectifier chamber is 0.5D. The two cavities are connected with flanges, and the FC is also connected

to the pipeline with flanges as a whole, which is convenient for installation, disassembly and maintenance, as shown in Figure 1.

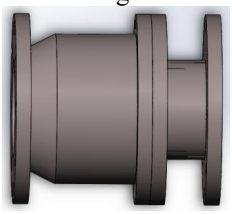

a. front view

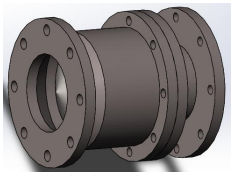

b. left view

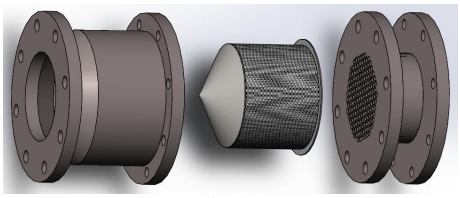

c. Split diagram

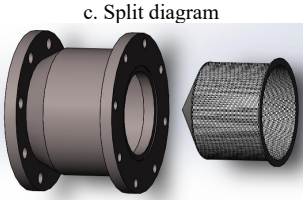

d. The filter cylinder is connected to the flanges

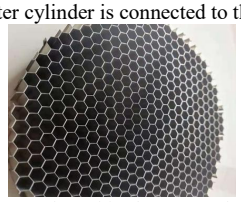

e. The honeycomb panel used in the rear end rectifying chamber

Figure 1: Self-designed combined FC

The flow inlet at the front of the FC adopts the design form of V-shaped diversion cone. The diameter of the filter buffer cavity is 1.25*D*, slightly larger than the diameter of the pipe *D*. Regardless of the flow state at the front, the inlet air flows into the filter buffer cavity along the diversion cone will be redistributed here to eliminate the flow field distortion. The design idea of diversion cone comes from V-cone flowmeter. As a differential pressure flowmeter, the V-cone flowmeter uses the annular throttling effect produced by the V-cone in the flow field to measure the flow rate by detecting the pressure difference between upstream and downstream. The V-cone itself acts as a rectifier for the flow field and significantly reduces the permanent pressure loss compared to throttling components such as orifice plates or venturi tubes. Therefore, in the front-end of the combined FC, the design of the V-shaped deflector cone and the enlarged diameter rectification cavity is very beneficial to reduce the pressure loss.

A filter screen is connected behind the diversion cone. On the one hand, the filter screen can filter the impurities in the gas medium to prevent the accumulation of dirt at the probe of the ultrasonic flowmeter and affect the transmission of signals. On the other hand, the gas flow pattern can be further adjusted. The diversion cone is connected with the filter screen to form a filter cylinder, which is connected with the flange at the outlet of the filter buffer chamber in the form of a slot, as shown in Figure 1d, which is very easy to disassemble and clean.

The rear rectifier cavity is made of metal honeycomb flow conditioner (as shown in Figure 1e), which is also manufactured in the form of flange wrapping, which has sufficient compressive strength. The airflow distribution enters the honeycomb flow conditioner after preliminary adjustment in the filter buffer cavity to obtain the ideal flow velocity distribution state.

3. Flow adjustment effect verification

In order to verify the flow adjustment effect of the combined FC, further simulation calculations were carried out and compared with the flow adjustment effect of the plate-type FC. In this paper, two basic pipeline layouts are selected for turbulence testing after model simplification(as shown in Figure 3), and the flow velocity distribution downstream of different kinds of FC is analyzed[7].

- An elbow is used as an upstream component to evaluate the effects of strong secondary flow and asymmetric velocity distribution.
- Two closely connected 90° double elbows, not in the same plane, are used as upstream components to evaluate the effects of moderate swirl and asymmetric velocity distributions.

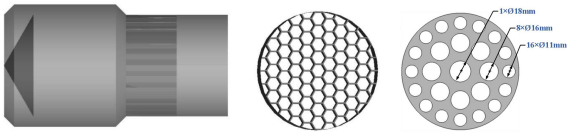

a. The combined FC b. The honeycomb panel c. The plate-type FC

Figure 2: Simplified schematic diagram of self-designed combined FC.

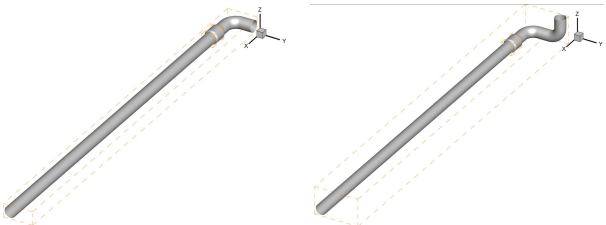

Figure 3: Simplified schematic diagram of pipeline layout.

The DN100mm fluid 3D model is established by SolidWorks software. The downstream cross section of the FC is located in the YZ plane, the center of the downstream cross section is the origin O, the pipe center line is located as the X axis, and the positive direction of the X axis is the downstream direction. ICEM software meshes the model, and finally imports it into FLUENT software for numerical iterative solution. Through the

solution results, the downstream velocity information of the FC can be obtained.

3.1 Flow adjustment effect verification downstream the single elbow

Due to the existence of the elbow, when the gas flows in the elbow, the gas flow rate and the pressure received are not uniformly distributed along the flow, causing the downstream flow field to be distorted, as shown in Figure 4a.

After installing the plate-type FC, along with the flow of the fluid, the velocity distribution gradually becomes stable, close to the fully developed state, and the lateral flow v_y and radial flow v_z basically disappear at 15D, but at about 20D, the flow velocity distribution is still off-axis and has not fully recovered to a fully developed state, as shown in Figure 4b.

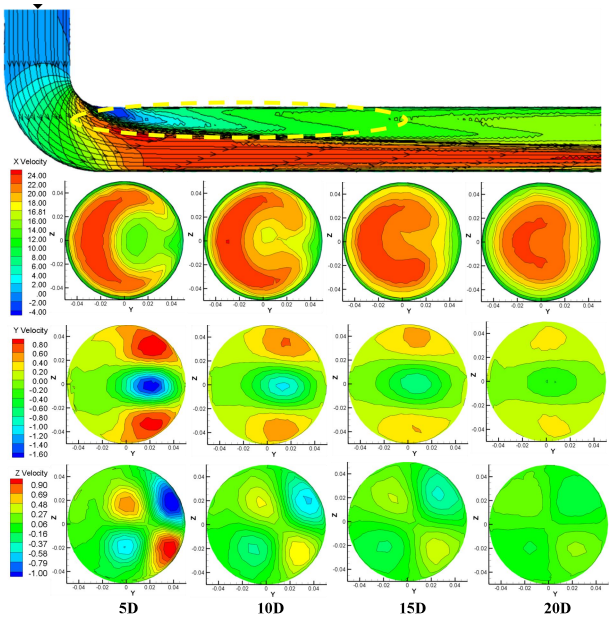

a. Flow field distribution downstream of single elbow

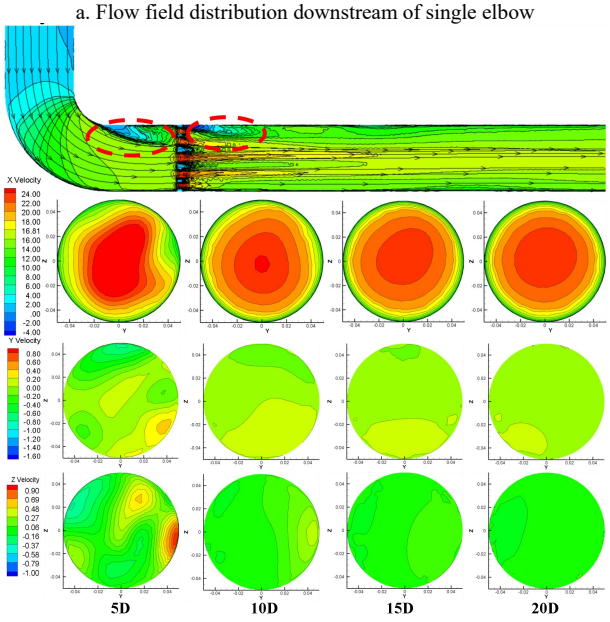

b. Flow field distribution downstream of plate-type FC

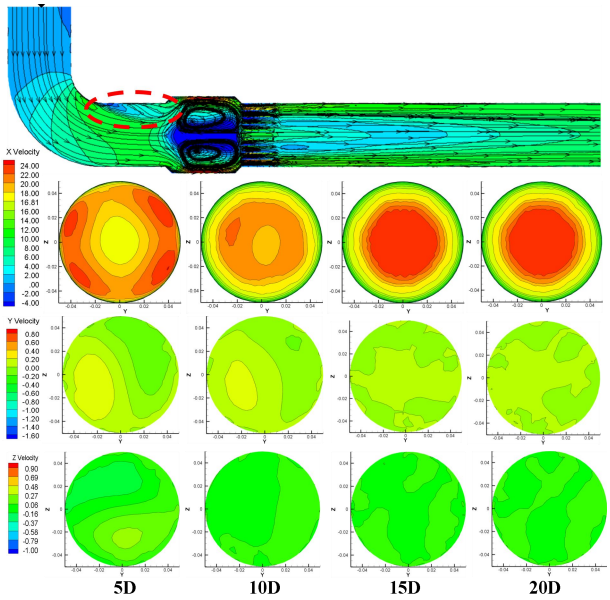

c. Flow field distribution downstream of combined FC

Figure 4: Comparison of downstream flow field distribution of single elbow under different installation conditions

The combined FC is more effective than the plate-type FC in eliminating lateral flow and radial flow. When it reaches at about 15D, the flow field distortion caused by the elbow can be completely eliminated, and the velocity v_x on the pipeline axis has recovered to a fully developed state, and the lateral flow v_y and radial flow v_z have also disappeared, as shown in Figure 4c.

3.2 Flow adjustment effect verification downstream the different-face double elbow.

Downstream of the different-sided double elbow, due to the superposition of the vortex area, the strength of the vortex and the lateral flow and radial flow are stronger than those of the single elbow, as shown in Figure 5a,

As a result, the vortex intensity at 10D downstream of the plate-type FC is still significant, making the velocity profile of axial flow v_x on the characteristic diameter deviate from the axis, and the transverse flow v_y and radial flow v_z are also obvious. As shown in Figure 5b, the fluid flow basically recovers to the fully developed state at about 20D.

The strong vortex flow in the distorted flow field makes the flow field distribution at 10D downstream of the combined FC still asymmetric. But also due to the structural design advantages of the combined FC, its effect in eliminating lateral flow and radial flow is more significant than that of the plate-type FC. At about 15D, the velocity v_x on the axis of the pipeline has recovered to a fully developed state, and the lateral flow v_y and radial flow v_z have also disappeared, as shown in Figure 5c.

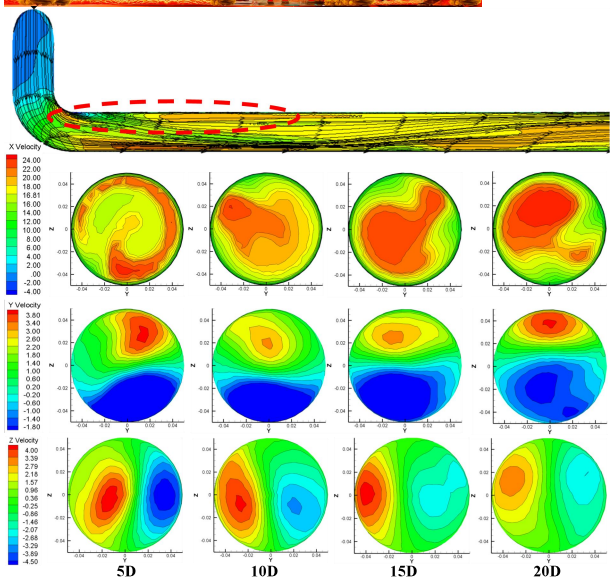

a. Flow field distribution downstream of double elbow.

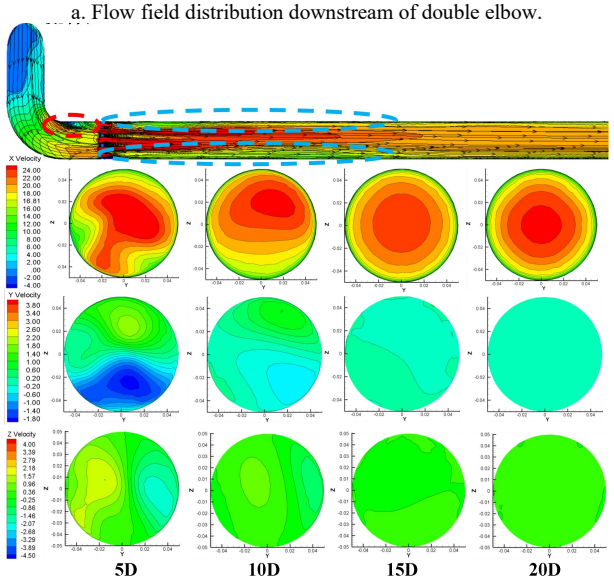

b. Flow field distribution downstream of plate-type FC.

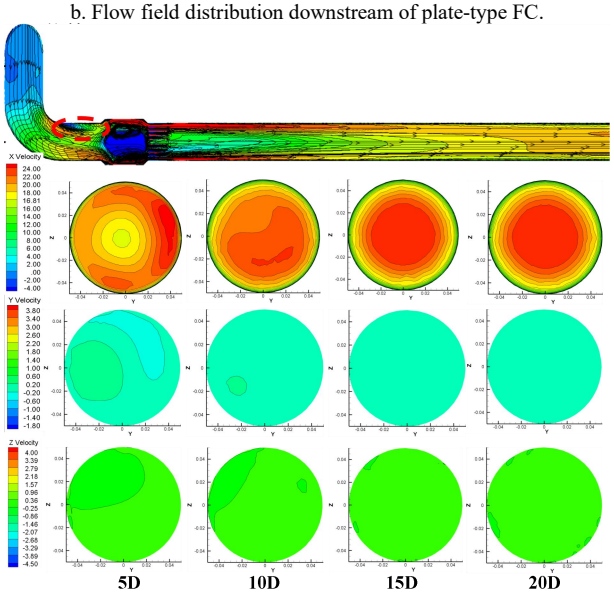

c. Flow field distribution downstream of combined FC

Figure 5: Comparison of downstream flow field distribution of double elbow under different installation conditions.

In this paper, a flow effect evaluation method is proposed. According to the simulation results in FLUENT, the surface-line-point method is used to obtain the flow velocity distribution on each section, different characteristic diameters on the same section, and different flow velocity sampling points on the same section in the downstream pipeline of the rectifier, and then calculate the flow velocity error. The sampling method is shown in Figure 6. In order to ensure that the flow velocity extracted by sampling can better reflect the distribution law of flow velocity downstream of the FC, the determination of the sampling method should follow the principles of uniform location distribution and consistent distribution in each cross section:

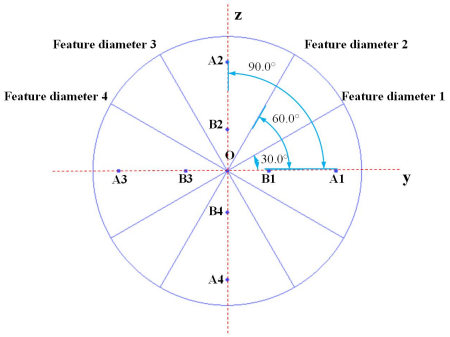

Figure 6: Determination of sampling points in downstream cross section of FC.

Figure 7 and Figure 8 respectively show the flow velocity distribution on the characteristic diameter when the plate-type FC and the combined-type FC are installed downstream of the different-sided double-elbow[8, 9].

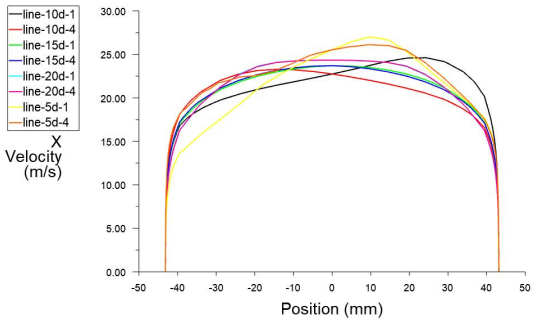

a. v_x—Characteristic Diameter 1/4

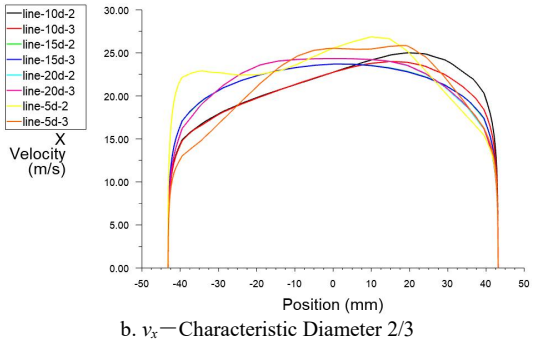

b. v_x—Characteristic Diameter 2/3

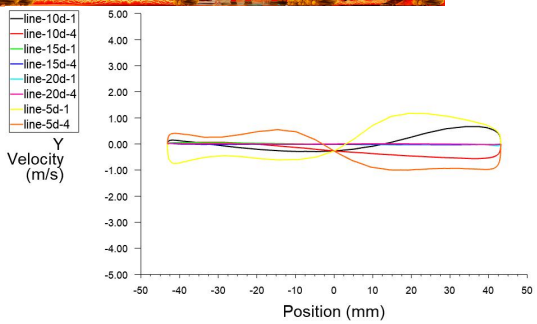

c. v_y—Characteristic Diameter 1/4

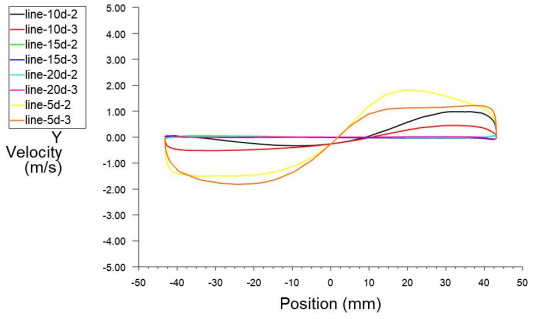

d. v_y—Characteristic Diameter 2/3

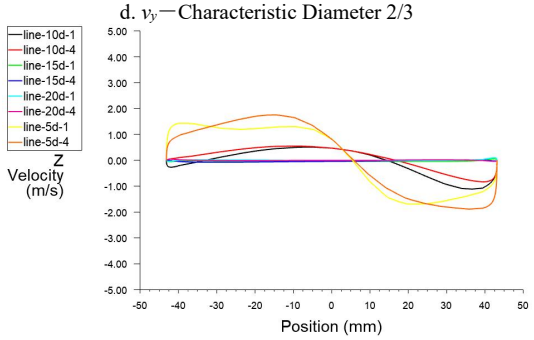

e. v_z—Characteristic Diameter 1/4

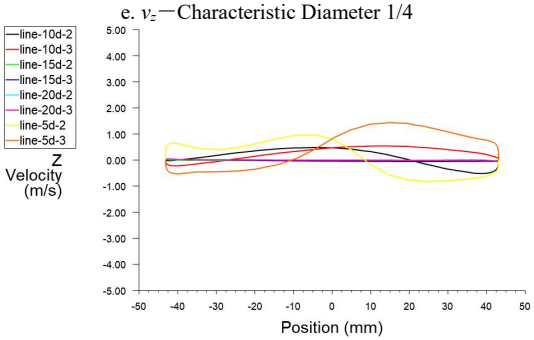

f. v_z—Characteristic Diameter 2/3

Figure 7: Velocity distribution over characteristic diameter when a plate-type FC is installed downstream of a double elbow.

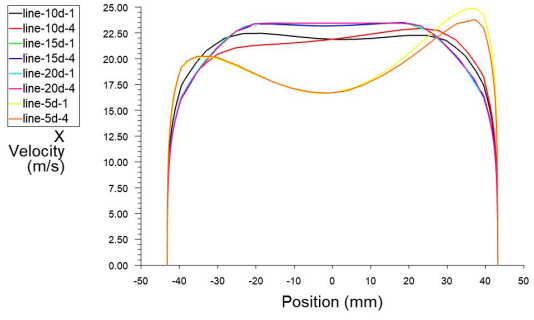

a. v_x—Characteristic Diameter 1/4

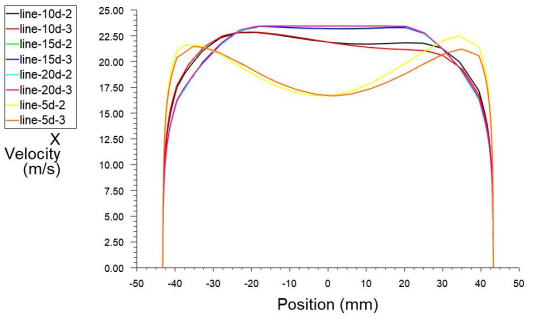

b. v_x—Characteristic Diameter 2/3

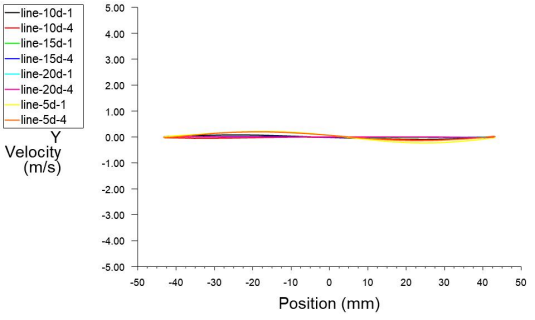

c. v_y—Characteristic Diameter 1/4

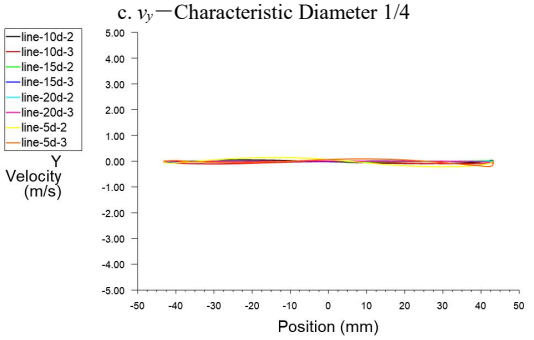

d. v_y—Characteristic Diameter 2/3

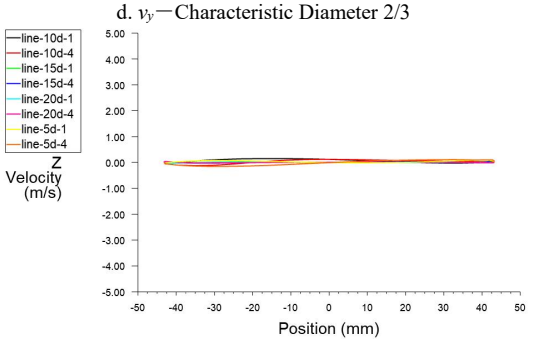

e. v_z—Characteristic Diameter 1/4

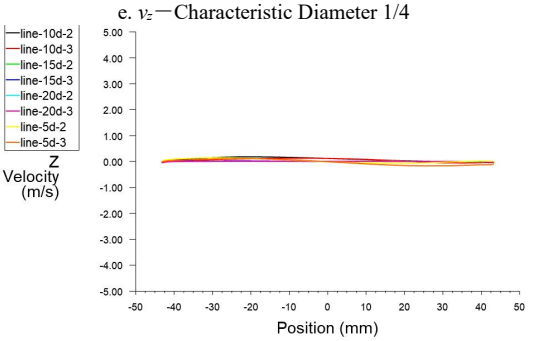

f. v_z—Characteristic Diameter 2/3

Figure 8: Velocity distribution over characteristic diameter when a combined-type FC is installed downstream of a double elbow.

As can be seen from the change in velocity profile, the combined FC has a significant advantage in

eliminating swirl and cross flow compared to the plate-type FC.

4. Optimization of design parameters

After comparing the flow adjustment effect of the combined FC, its structure was further optimized.

In the combined FC, the honeycomb panels used in the rear rectifier cavity are industrial finished products and have no special design requirements, so the structure of the rear rectifier cavity can be determined. The design focus is on the front filter buffer chamber, including the following influencing factors:

1. Whether the filter buffer cavity is designed for diameter expansion;

2. The size of the cone angle α of the V-shaped deflector cone;

3. The size of throttle ratio β of V-shaped deflector cone.

Here, the throttling ratio β is defined as the equivalent diameter ratio of the cone, that is, the ratio of the annular flow area S_A to the pipe cross-sectional area S_B, as shown in Figure 9:

$$\beta = \frac{S_A}{S_B} = \sqrt{\frac{\frac{\pi D^2}{4} - \frac{\pi d^2}{4}}{\frac{\pi D^2}{4}}} = \sqrt{\frac{D^2 - d^2}{D^2}} \quad (1)$$

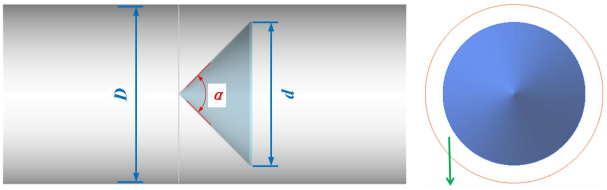

Figure 9: Schematic diagram of related parameters of the deflector cone.

By comparing the flow velocity v_i at the sampling point with the flow velocity v_i' in the fully developed state, the flow velocity errors of 9 sampling points in each section downstream of the FC are calculated and accumulated, and the accumulated flow velocity error $\boldsymbol{E}_{\text{surface}}$ in the same section is obtained:

$$E_{\text{surface}} = \sum_{i=1}^{n} \left| \frac{v_i - v'_i}{v'_i} \right| \times 100\% \quad (2)$$

Taking the pipe diameter D as the interval distance, a total of 26 characteristic points on the section from the outlet 5D to the downstream 30D of the FC are selected to calculate the flow velocity error. The accumulated flow velocity error in the same section can reflect the flow velocity distribution in each cross section, which is convenient to determine the installation position of the flowmeter downstream of the FC. The smaller the Es_{surface}, the higher the full development of the flow velocity in the corresponding section downstream of the FC, and the better the flowmeter is installed near the section.

4.1 The influence of expanding or not on the flow adjustment effect.

When the upstream is a double elbow with different sides, taking the diversion cone angle α=120°, equivalent diameter ratio β=0.6, the influence of whether the filter buffer chamber is a diameter expanding design on the flow adjustment effect is compared under the same parameters, and the adjustment effect is compared through the accumulated velocity error in each characteristic plane downstream, as shown in Figure 10.

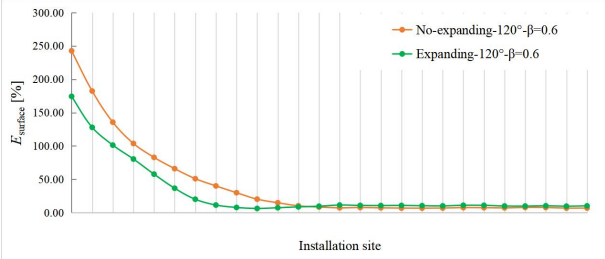

Figure 10: The influence of expanding or not on the flow adjustment effect.

As can be seen from the simulation results, when the filter rectifying chamber is an expanding pipe, the cumulative velocity error in each characteristic plane of the downstream tends to be stable when it is about 12D-13D, while when the filter rectifying chamber is designed as a non-expanding pipe, i.e. straight pipe, the cumulative velocity error tends to be stable when it is about 16D. The effect of the expanding tube is better.

4.2 Influence of cone angle α of V-shaped deflector cone

Take the equivalent diameter ratio β=0.6, and optimize the selection of the deflector cone angle α under the condition of non-expanded straight pipes: take α=120°, α=90° and α=60° respectively to compare the rectification effect , and also compare the rectification effect with the accumulated flow velocity error in each characteristic plane downstream, and the comparison results are shown in Figure 11.

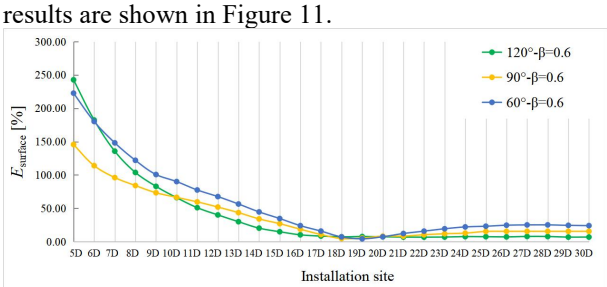

Figure 11: Influence of cone angle α of V-shaped deflector cone

In general, the larger the cone angle α of the deflector cone downstream of the combined flow conditioner, the better the flow adjustment effect. This is due to the fact that the larger the cone angle of the deflector cone encountered by the distorted fluid, the more it can recover to a fully developed state in a shorter distance downstream.

4.3 Influence of V- shaped cone throttling ratio β size

The selection of equivalent diameter ratio β was optimized under the condition that the cone angle α of the straight pipe and diversion cone without expansion was 90°: β=0.8, β=0.6 and β=0.45 were taken to

compare the flow adjustment effect, and the cumulative velocity error in each characteristic plane downstream was also used to compare the flow adjustment effect, as shown in Figure 12. The results show that when the cone angle is 90° , the flow adjustment effect is best when the equivalent diameter ratio β=0.45.

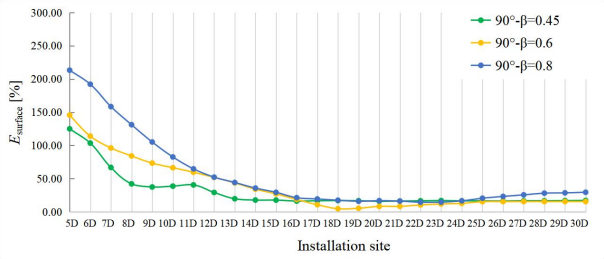

Figure 12: The effect of equivalent diameter ratio β on the flow adjustment effect of non-expanding pipe and cone Angle of 90°

The selection of equivalent diameter ratio β was optimized under the condition that the filter buffer chamber was taken as the expanding pipe and the cone angle α of the diversion cone was 120° : β=0.8, β=0.6 and β=0.45 were also taken to compare the flow adjustment effect, as shown in Figure 13. The results show that when the cone angle is 120°, the flow adjustment effect is best when the equivalent diameter ratio β=0.6.

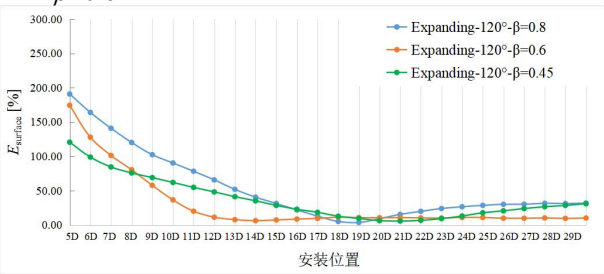

Figure 13: The effect of equivalent diameter ratio β on the flow adjustment effect of expanding pipe and cone Angle of 120° .

It can be seen that the flow adjustment effect is better when the filter buffer cavity is an expanding tube, the diversion cone angle α is 120°, and the equivalent diameter ratio β is 0.6.

5. Conclusion

In view of the current situation that the flow conditioners used in combination with various ultrasonic flowmeters on the market are relatively specific, and the applicability analysis of flow conditioner with different structures to different flow types is still lacking, this paper proposes a design scheme of combined flow conditioner and a flow field distribution evaluation method.

In this paper, a flow effect evaluation method is proposed. A surface-line-point method is used to obtain the flow velocity distribution on each section, different characteristic diameters on the same section, and different flow velocity sampling points on the same section in the downstream pipeline of the FC, and then calculate the flow velocity error.

Simulation results show that when the filter buffer cavity of the combined FC is an expanding tube, the cone angle of the V-shaped deflector cone is 120° , and the equivalent diameter ratio is 0.6, the flow adjustment effect is the best.

References

[1]. Chen W. G. Analysis and compensation method of non-ideal flow field for ultrasonic gas flowmeter[D]. Hangzhou: Zhejiang University, 2015.

[2]. Chao Z. H., Hui P. L., Stephane S. A., et al. CFD Aided Investigation of Multipath Ultrasonic Gas Flow Meter Performance Under Complex Flow Profile[J]. IEEE Sensors Journal, 2014, 14 (3): 897-907.

[3]. Lin Q., Chen Z. X., Zhang Y. Y., et al. Overview of ultrasonic flowmeter and numerical simulation of flow field[J]. Technology Supervision in Petroleum Industry, 2018, 34 (11): 43-47.

[4]. ASME PTC18-2011_Hydraulic Turbines and Pump-Turbines Performance Test Codes[S]. American Society of Meehanieal Engineers, 2011.

[5]. Liu E. B., Tan H., Peng S. B. A CFD simulation for the ultrasonic flow meter with a header[J]. Tehnicki Vjesnik-Technical Gazette, 2017, 24 (6): 1797-1801.

[6]. Brown G. J., Jnr W. R. F. Qualification Testing of an 8-path Ultrasonic Gas Meter[C]. In 32nd International north sea flow measurement workshop, 2014.

[7]. Hallanger A., Frøysa K. E., Lunde P. CFD-simulation and installation effects for ultrasonic flow meters in pipes with bends[J]. International Journal of Applied Mechanics & Engineering, 2002, 7 (1).

[8]. Hallanger A., Saetre C., Frøysa K. E. Flow profile effects due to pipe geometry in an export gas metering station – analysis by CFD simulations[J]. Flow Measurement and Instrumentation, 2018, 61: 56-65.

[9]. Crawford N., Spence S., Simpson A., et al. A numerical investigation of the flow structures and losses for turbulent flow in 90° elbow bends[J]. Journal of Process Mechanical Engineering, 2009, 223 (1): 27-44.